α-Hydrogen Abstraction by •OH and •SH Radicals From Amino Acids and Their Peptide Derivatives

Bun Chan,*[,†,§] Amir Karton,[¶] Christopher J. Easton[‡,§] and Leo Radom*[,†,§]

[†] School of Chemistry, University of Sydney, Sydney, NSW 2006, Australia

[§] ARC Centre of Excellence for Free Radical Chemistry and Biotechnology

[¶] School of Chemistry and Biochemistry, University of Western Australia, Perth, WA 6009, Australia

[‡] Research School of Chemistry, The Australian National University, Canberra, ACT 2600, Australia

Abstract: We have used computational quantum chemistry to investigate the thermochemistry of α-hydrogen abstraction from the full set of amino acids normally found in proteins, as well as their peptide forms, by •OH and •SH radicals. These reactions, with their reasonable complexity in the electronic structure (at the α-carbon), are chosen as a consistent set of models for conducting a fairly robust assessment of theoretical procedures. Our benchmarking investigation shows that, in general, the performance for the various classes of theoretical methods improves in the order: non-hybrid DFT ◘ hybrid DFT ◘ double-hybrid DFT ◘ composite procedures. More specifically, we find that the DSD-PBE-P86 double-hybrid DFT procedure yields the best agreement with our high-level W1X-2 barriers and reaction energies for this particular set of systems. A significant observation is that, when one considers relative instead of absolute values for the barriers and reaction energies, even non-hybrid DFT procedures perform fairly well. In order to exploit this feature in a cost-effective manner, we have examined a number of multi-layer schemes for the calculation of reaction energies and barriers for the abstraction reactions. We find that accurate values can be obtained when a "core" of glycine plus the abstracting radical is treated by DSD-PBE-P86, and the substituent effects are evaluated with M06-2X. Inspection of the set of calculated thermochemical data shows that the correlation between the barriers and reaction energies is strongest when the reactions are either endergonic or near-thermoneutral.

Introduction

Hydrogen-atom abstraction from amino acid residues in peptides and proteins is a critical event that may lead to fragmentation of the peptide chains.[1] Such degradation processes are associated with pathological conditions including ageing, cancer, and neurodegenerative disorders.[2] In general, the fragmentation occurs more readily from backbone α-radicals. From a biological perspective, it is relevant that, although α-radicals are often subject to large stabilization associated with captodative interactions,[3] as reflected for example in the calculated α-C–H bond dissociation enthalpies of the natural amino acids,[3b,d,4] α-hydrogens are in fact, remarkably, quite inert towards abstraction by electrophilic radicals.[5]

The contrathermodynamically slow α-abstraction is often rationalized in terms of so-called "polar effects".[6] Thus, the σ-electron-withdrawing nature of the α-substituents renders the α-carbon electron deficient. This, coupled with electrophilic attacking radicals (e.g., •Cl), results in a destabilization of the α-transition structure.[7] Although α-abstraction reactions are, arguably, of less biological relevance than side-chain reactions because they occur less frequently, they are of interest from the perspective of quantum chemistry computations. The α-radicals (and the transition structures that lead to their formation), with their direct interactions with both the amino and carboxyl substituents, represent a system that may potentially be challenging for theoretical methods.

In a series of studies,[8] we have used computational quantum chemistry to investigate the fundamentals of the polar effect in relation to hydrogen abstraction from amino acid derivatives. In two of these earlier studies,[8a,c] we have identified, for the specific case of hydrogen abstraction by Cl•, theoretical methods suitable for the reliable calculation of barriers and reaction energies. Since the publication of these studies, the continuing rapid development of computational chemistry methodologies has led to the emergence of numerous more advanced procedures.[9] We therefore feel that it is now appropriate to carry out a new benchmark study, in

order to evaluate and, if necessary, modify our previous recommendations as to the most reliable protocols for the study of these reactions.

In the present study, we examine α-abstraction by •OH and •SH radicals from the twenty amino acids [NH_2–CH(R)–C(=O)OH] normally found in proteins, and their peptide derivatives [CH_3C(=O)NH–CH(R)–C(=O)NHCH_3]. These systems represent a diverse set of test cases that may pose potential challenges to quantum chemistry procedures. In addition, they broaden the assessment set used previously,[8] and thus serve as an independent probe for the reliability of the theoretical methodologies. We also aim to provide our best estimated thermochemical values for these reactions using the method that we identify as most appropriate from our benchmark study, and we hope that these values complement studies into the theoretical thermochemistry of radicals.[10]

Computational Details

Standard ab initio molecular orbital theory and density functional theory (DFT) calculations[11,12] were carried out with Gaussian 09[13] and ORCA 3.1.[14] In our previous studies, we have recommended the use of BHandHLYP/6-31+G(d,p) for geometry optimization and subsequent vibrational frequency calculations. We have also advocated the use of the IRCmax procedure[15] in conjunction with the B2K-PLYP method[16] and a double-ζ basis set to ensure reliable transition structure geometries. We note, however, that the IRCmax procedure only has a significant effect in a small number of the cases that we have examined previously.

We regard density-functional theory (DFT) methods to be generally quite reliable for geometry optimizations for minima and for the coordinates in the transition structures that are orthogonal to the reaction path. In addition, the reaction path can be further refined with the IRCmax procedure if necessary. Furthermore, considering the overall accuracy of thermochemical quantities obtained with scaled DFT frequencies, we believe that our previous recommendations still represent a good approach to this end. Thus, in the present study, we focus on the assessment of single-point energies obtained with a variety of theoretical procedures. For the

benchmark, we initially obtain the geometries and associated thermochemical quantities with the BHandH-LYP/6-31+G(d,p) procedure without the application of IRCmax. Zero-point vibrational energies (ZPVEs), and thermal corrections for enthalpies (ΔH_{298}) and entropies (S_{298}) were obtained with scaled BHandH-LYP/6-31+G(d,p) vibrational frequencies with appropriate literature scale factors.[17] The effect of using IRCmax is subsequently included in the determination of our final values for the barriers and reaction energies using the most appropriate methods that emerge from the benchmark study.

There are potentially a large number of conformers to consider for amino acids and peptides. To this end, a recent comprehensive computational study has identified the low-energy conformers for the peptide derivatives [$CH_3C(=O)NH–CH(R)–C(=O)NHCH_3$] of the twenty amino acids normally found in proteins.[18] In the present study, we employ these conformations in the starting geometries for optimizations of not only the peptides themselves but also the associated transition structures and product radicals. Such a choice is based on the consideration of the potential structural rigidity of amino acid residues in enzymes, such that the probability of substantial conformational changes in going from substrate to product is reduced. It is also important to note that the lowest-energy conformations would depend on the level of theory, and the conformations determined in the recent study,[18] which we employ, may not be the lowest when obtained with different methods.

In order to enable the use of higher-level theoretical procedures to obtain benchmark energies, in addition to the peptides, we also examine the (smaller) neutral amino acids [$NH_2–CH(R)–C(=O)OH$]. In these cases, the initial geometries were obtained by truncating the peptide structures. We note that the amino acids may in some cases have rather different low-energy conformations when compared with the peptides. However, for benchmark purposes, we prefer to maximize the applicability of the results from the amino acids to the peptides, and therefore to maintain similar conformations between the two sets of systems.

We examine a representative set of theoretical procedures in our benchmark study. These include W1X-2,[19] which is used as our highest benchmark level, the composite procedures G4,[20] G4(MP2)-6X,[21] G4(MP2),[22] G3X(MP2)-RAD[23] and CBS-QB3,[24] the double-hybrid density functional theory (DH-DFT) procedures B2K-PLYP,[16] PWP-B95-D3,[25] DuT-D3[26] and DSD-PBE-P86,[27] the hybrid DFT methods PW6-B95,[28] ωB97X[29] and M06-2X,[30] and the non-hybrid functionals M06-L[31] and MN12-L.[32] This set of methods is chosen as they have already been widely shown to be rather accurate in many cases, including in our own benchmark studies of radical reactions.[33,34,35] We thus deemed it very likely that at least some of them would provide good accuracy for the systems in the present study. For the DH-DFT methods, the aug'-cc-pVTZ+d basis set was used. For the hybrid and non-hybrid functionals, we have employed the somewhat smaller 6-311+G(3df,2p) basis set.

Results and Discussion

Assessment of Theoretical Procedures with Neutral Amino Acids. We were able to obtain barriers and reaction energies for α-hydrogen abstraction by the •OH radical with the high-level W1X-2 procedure for nine of the twenty amino acids, namely Ala, Asn, Asp, Cys, Gly, Pro, Ser, Thr and Val. These are employed as our primary benchmark for the lower-level theoretical procedures. The results are shown in Table 1 (barriers) and Table 2 (reaction energies).

It can be seen that, for the barriers, the overall performance of the various classes of procedures improves in the order: non-hybrid DFT ◘ hybrid DFT ◘ double-hybrid DFT ◘ composite procedures. Among the five composite procedures, CBS-QB3, G4(MP2)-6X and G4 have comparable performance, with mean absolute deviations (MADs) from benchmark values of 3.4, 3.9 and 3.4 kJ mol^{-1}, respectively. The MAD of 6.1 kJ mol^{-1} for G4(MP2) and that for G3X(MP2)-RAD (7.5 kJ mol^{-1}) are notably larger. Among the four DH-DFT methods, DSD-PBE-P86, having an MAD of just 3.0 kJ mol^{-1}, is the best performer for this set of systems. The other three double-hybrid procedures all have MADs of ~ 7–10 kJ mol^{-1}.

Table 1. Mean Absolute Deviations (MAD), Mean Deviations (MD), Standard Deviations (SD) of the Deviations, and Largest Deviations (LD) in kJ mol^{-1} for the Various Theoretical Procedures From W1X-2 Benchmark Vibrationless Barriers for α-Hydrogen Abstraction by the •OH Radical from Nine Amino Acids[a]

	MAD	MD	SD	LD
		Composite procedures		
G4	3.4	–3.4	2.4	–6.6
G4(MP2)-6X	3.9	3.9	1.4	5.7
G4(MP2)	6.1	–6.1	3.5	–10.6
G3X(MP2)-RAD	7.5	7.5	0.7	8.4
CBS-QB3	3.4	–3.4	0.6	–4.4
		Double-hybrid DFT		
B2K-PLYP	7.9	7.9	0.9	9.3
PWP-B95-D3	9.7	–9.7	1.3	–11.7
DuT-D3	7.0	7.0	1.6	9.0
DSD-PBE-P86	3.0	3.0	0.6	4.2
		Hybrid DFT		
PW6-B95	19.8	–19.8	2.5	–23.3
ωB97X	9.2	–9.2	1.2	–10.9
M06-2X	4.6	–4.6	1.1	–6.6
		Non-hybrid DFT		
M06-L	33.6	–33.6	2.7	–36.7
MN12-L	6.0	–6.0	2.2	–9.6

[a] Ala, Asn, Asp, Cys, Gly, Pro, Ser, Thr and Val.

Table 2. Mean Absolute Deviations (MAD), Mean Deviations (MD), Standard Deviations (SD) of the Deviations, and Largest Deviations (LD) in kJ mol^{-1} for the Various Theoretical Procedures Against W1X-2 Benchmark Vibrationless Reaction Energies for α-Hydrogen Abstraction by the •OH Radical from Nine Amino Acids[a]

	MAD	MD	SD	LD
		Composite procedures		
G4	2.5	–2.5	1.3	–4.5
G4(MP2)-6X	1.6	1.6	0.6	2.5
G4(MP2)	5.5	–5.5	2.4	–8.4
G3X(MP2)-RAD	6.7	6.7	1.0	8.1
CBS-QB3	2.6	–2.6	0.5	–3.6
		Double-hybrid DFT		
B2K-PLYP	1.6	–1.6	0.8	–2.9
PWP-B95-D3	5.9	–5.9	1.0	–7.1
DuT-D3	2.8	–2.8	0.6	–4.0
DSD-PBE-P86	1.9	1.9	0.5	2.7
		Hybrid DFT		
PW6-B95	16.9	–16.9	2.1	–18.7
ωB97X	6.0	–6.0	1.2	–7.4
M06-2X	5.7	–5.7	0.9	–7.3
		Non-hybrid DFT		
M06-L	10.2	–10.2	3.4	–14.0
MN12-L	7.7	–7.7	3.1	–11.7

[a] Ala, Asn, Asp, Cys, Gly, Pro, Ser, Thr and Val.

While all the composite protocols and DH-DFT methods perform fairly well, the hybrid and non-hybrid DFT procedures show considerable variation in their performance. Thus, among the hybrid DFT methods, M06-2X has an MAD of just 4.6 kJ mol^{-1}, whereas the MAD for PW6-B95 is 19.8 kJ mol^{-1}. Likewise, for the two non-hybrid DFT procedures, the MAD of 6.0 kJ mol^{-1} for MN12-L is fairly small, but that

for M06-L is considerably larger (33.6 kJ mol^{-1}). It is noteworthy that, for all methods among all classes, the mean deviation (MD) values have the same magnitudes as the corresponding MADs. Thus, the deviations are quite consistent in their directions. Such a systematic behavior is reflected in the small standard deviation (SD) values for the deviations, which are less than 4 kJ mol^{-1}. The latter observation also implies the prospect of a good performance for the calculation of *relative* barriers with all methods, which will be discussed later.

For the reaction energies, the general observations are similar to those for barriers. However, the MADs are typically smaller. We again see that deviations are quite systematic, as reflected in the same magnitude of the MDs and the corresponding MADs. The SD values, like those for the barriers, are also quite moderate for the reaction energies. Overall, for both the calculation of barriers and reaction energies, taking into account the accuracy and the computational efficiency, we deem DSD-PBE-P86 to be the most appropriate method for the investigation of the systems in the present study. We also note that the MN12-L procedure is computationally inexpensive yet has a performance that seems to rival methods that are much more computationally demanding for this particular set. It may therefore provide a cost-effective means for the study of similar systems that are considerably larger.

Validation on Peptides: Absolute Barriers and Reaction Energies. We now examine further a subset of the theoretical procedures for their performance in the calculation of barriers and reaction energies for hydrogen abstraction by •OH and •SH from the α-position of peptide derivatives of the amino acids, with the general structure $CH_3C(=O)NH–CH(R)–C(=O)NHCH_3$. For this set of systems, the use of the W1X-2 protocol is computationally prohibitive with our available resources in almost all cases. We thus use the DSD-PBE-P86 procedure to obtain our benchmark values.

We note that the good performance of DSD-PBE-P86 observed for •OH abstraction from the smaller set of neutral amino acids may not necessarily lead to

equally good performance for a more diverse set of somewhat different systems. However, if there is good agreement between several medium- to high-level procedures of different types, this would suggest a degree of robustness in the calculated values. As a result, we have examined the G4(MP2)-6X, B2K-PLYP, DuT-D3, ωB97X, M06-2X and MN12-L procedures alongside DSD-PBE-P86. We will specifically assess the agreement between DSD-PBE-P86, the two other DH-DFT procedures, and G4(MP2)-6X, in order to assess the likely accuracy of the calculated barriers and reaction energies.

The MADs for the barriers and reaction energies are shown in Table 3. It can be seen that there is a fair agreement among the various DH-DFT procedures and between DH-DFT and G4(MP2)-6X. A major exception is for the •SH abstraction barriers obtained with B2K-PLYP, which we find to be systematically overestimated when compared with other DH-DFT methods. It is noteworthy that the MADs between DSD-PBE-P86 and G4(MP2)-6X for the barriers are just 3.6 and 1.5 kJ mol^{-1}, respectively, for •OH and •SH abstractions. While the large MAD of 6.0 kJ mol^{-1} for the •OH abstraction reaction energies for G4(MP2)-6X is disappointing, this can be traced largely to the difference in the HO–H bond dissociation energies obtained with DSD-PBE-P86 (487.2 kJ mol^{-1}) and G4(MP2)-6X (493.2 kJ mol^{-1}). It is noteworthy that the G4(MP2)-6X value in fact agrees better with the W1X-2 value of 498.1 kJ mol^{-1} and with the NIST experimental value[36] of 498.8 kJ mol^{-1} than does the DSD-PBE-P86 one. Thus, the very good agreement between DSD-PBE-P86 and W1X-2 for the amino acids (Table 1 and Table 2) is likely to involve some fortuitous but consistent cancellation of deviations.

Table 3. Mean Absolute Deviations (MAD, kJ mol^{-1}) From DSD-PBE-P86 Vibrationless Barriers and Reaction Energies for α-Hydrogen Abstraction by the •OH and •SH Radicals from the Peptide Derivatives of the Twenty Amino Acids

	Barrier		Reaction energy	
	•OH	•SH	•OH	•SH
G4(MP2)-6X	3.6	1.5	6.0	2.8
B2K-PLYP	6.7	11.6	1.9	0.5
DuT-D3	0.8	6.1	2.9	0.4
ωB97X	6.5	5.4	4.9	7.5
M06-2X	6.3	1.4	4.9	2.8
MN12-L	5.4	11.5	11.5	20.9

For the two hybrid DFT methods, the performance across the four sets of quantities is generally reasonable, with MAD values that are well below 10 kJ mol^{-1} in all cases. MN12-L, despite its good performance for the barriers for abstraction by •OH, does not perform very well for •SH abstraction barriers and for both •OH and •SH abstraction reaction energies. Its performance for the reaction energies for •SH abstraction is particularly poor, with an MAD of 20.9 kJ mol^{-1}. To this end, we note that MN12-L in fact gives an HS–H bond energy (384.7 kJ mol^{-1}) that is quite close to the W1X-2 and experimental values of 382.6 and 381.7 kJ mol^{-1}, respectively. On the other hand, DSD-PBE-P86 gives a value of 374.9 kJ mol^{-1}, which has a somewhat larger deviation from the W1X-2 and experimental values and, notably, is smaller than the MN12-L value by 9.8 kJ mol^{-1}. This suggests the existence of residual differences between the two methods that are associated with the amino acid radical/amino acid pairs. Indeed, the bond dissociation energies for the peptides are consistently being underestimated by MN12-L when compared with DSD-PBE-P86, with an MD of –11.1 kJ mol^{-1} and a range of –6.3 to –16.1 kJ mol^{-1} for the deviations.

Relative Barriers and Reaction Energies. As mentioned in the previous section, the deviations from benchmark values for •OH abstraction from the neutral amino acids

are quite systematic (Table 1 and Table 2) for all procedures examined. As a result, one can reasonably expect improved performance for the calculation of relative barriers and relative reaction energies, regardless of the method employed. To investigate the extent of such an improvement, we have obtained barriers and reaction energies for peptide derivatives of other amino acids relative to those for glycine. The MADs from the DSD-PBE-P86 relative quantities are shown in Table 4.

Table 4. Mean Absolute Deviations (MAD, kJ mol^{-1}) From DSD-PBE-P86 (relative to glycine) Vibrationless Barriers and Reaction Energies for α-Hydrogen Abstraction by the •OH and •SH Radicals from Peptide Derivatives of the Twenty Amino Acids

	Barrier		Reaction energy	
	•OH	•SH	•OH	•SH
G4(MP2)-6X	3.0	3.1	1.5	1.5
B2K-PLYP	1.0	2.4	0.4	0.4
DuT-D3	0.4	1.3	0.5	0.5
ωB97X	1.3	1.1	2.2	2.2
M06-2X	0.8	1.1	1.0	1.0
MN12-L	2.0	2.3	3.3	3.3

It is apparent that the improvement in performance is significant for these systems. Remarkably, even for the relative reaction energies of •SH abstraction obtained with MN12-L, the MAD is just 3.3 kJ mol^{-1}, despite this method giving an MAD of 20.9 kJ mol^{-1} for the calculation of absolute reaction energies. Overall, for the calculation of relative barriers and relative reaction energies for these systems, the typical MADs are approximately 3 kJ mol^{-1} or smaller. In the next section, we explore the calculation of absolute quantities using a combination of high- and low-level methods by taking advantage of the good performance for relative quantities.

Absolute Quantities from Relative Barriers and Relative Reaction Energies. We now proceed to examine the calculation of barriers and reaction energies using a variety of multi-layer approaches. We will employ DSD-PBE-P86 as our target level, and apply a combination of high- and low-level theoretical procedures, respectively,

to the model and real systems, in order to approximate the target energies. The combination of high- and low-level methods are: DSD-PBE-P86/M06-2X, DSD-PBE-P86/MN12-L, and M06-2X/MN12-L (Table 5). The single (low-)level methods M06-2X and MN12-L are also included for comparison. It is noteworthy that the approaches examined in this section are, in spirit, quite similar to some formal multi-layer methodologies such as ONIOM.[37] The recommendations associated with the results here are therefore likely to be applicable in this context.

We first look at the application of these protocols to the approximation of the •OH abstraction barriers for the neutral amino acids (row A). In this case, glycine is used as the model system treated by the higher-level method, with the lower-level method employed to obtain the relative barriers, i.e., the substituent effect for the side chain in the abstraction reaction. For the DSD-PBE-P86/M06-2X protocol, the MAD from full DSD-PBE-P86 values is just 0.8 kJ mol^{-1}. The MAD of 1.5 kJ mol^{-1} for the somewhat more approximate DSD-PBE-P86/MN12-L method is only slightly larger. In contrast, when the higher-level method of DSD-PBE-P86 is replaced for the model system, the MAD becomes considerably larger for the three remaining methods. Similar behavior is observed when peptidic amino acids are modeled by peptidic glycine at the higher-level in conjunction with side-chain effects evaluated at the lower level, for both •OH (row B) and •SH (row C) abstractions.

Table 5. Mean Absolute Deviations (MAD, kJ mol^{-1}) From DSD-PBE-P86 Barriers and Reaction Energies for the Various Multi-Layer Protocols

	Real system	Model system	DSD-PBE-P86 /M06-2X	DSD-PBE-P86 /MN12-L	M06-2X	M06-2X /MN12-L	MN12-L
				Barriers			
A	amino acid/•OH	glycine/•OH	0.8	1.5	7.8	8.3	9.1
B	peptidic amino acid/•OH	peptidic glycine/•OH	0.8	2.1	6.2	6.0	5.1
C	peptidic amino acid/•SH	peptidic glycine/•SH	1.3	2.0	1.6	1.8	11.2
D	peptidic amino acid/•OH	glycine/•OH	1.3	3.8	6.2	4.5	5.1
E	peptidic amino acid/•SH	glycine/•SH	2.8	2.4	1.6	1.9	11.2
F	peptidic amino acid/•SH	glycine/•OH	8.9	3.1	1.6	10.4	11.2
				Reaction energies			
G	amino acid/•OH	glycine/•OH	1.6	5.9	8.2	12.5	11.1
H	peptidic amino acid/•OH	peptidic glycine/•OH	1.0	3.3	4.8	7.5	11.5
I	peptidic amino acid/•SH	peptidic glycine/•SH	1.0	3.3	2.8	5.4	20.9
J	peptidic amino acid/•OH	glycine/•OH	1.9	6.2	4.8	12.8	11.5
K	peptidic amino acid/•SH	glycine/•SH	1.9	6.2	2.8	10.7	20.9
L	peptidic amino acid/•SH	glycine/•OH	3.8	15.6	2.8	22.2	20.9

Rows D–F show the results for more drastic approximations of the real system. In all three cases, neutral glycine is used as the model system for peptides, with the lower-level theoretical method used not only to obtain the substituent effects for the side chain but also for the peptidic substitutions at both termini. For the results shown in row F, the lower level also approximates the difference between abstractions by the two different radicals (•OH and •SH). The DSD-PBE-P86/M06-2X protocol gives MADs of 1.3 and 2.8 kJ mol^{-1} when M06-2X is used to approximate the side-chain and terminal-peptide substituent effects for •OH and •SH abstractions, respectively (rows D and E). However, using M06-2X to further evaluate the effect of changing the abstracting radical (row F) leads to a notably larger MAD of 8.9 kJ mol^{-1}. This can be attributed to a consistent underestimation of the •OH abstraction barriers for the neutral amino acids by M06-2X, but a generally very good agreement of M06-2X with DSD-PBE-P86 for the •SH abstractions for the peptides (Table 3).

These results suggest that, as long as the "reactive core" of glycine plus the radical is preserved in the model system, and both the high- and low-level methodologies are sufficiently accurate, the results obtained with such a multi-level approach should be quite accurate. This is also seen to be the case for reaction energies, where the results qualitatively closely resemble those for barriers. Thus, for the study of α-hydrogen abstractions from peptides, we deem the use of the DSD-PBE-P86(for glycine plus the radical)/M06-2X(for the effect of substituents) to provide a reasonable means of obtaining barriers and reaction energies in a cost-effective manner.

As noted earlier, the multi-layer approaches presented here are similar to some of the more formal methodologies such as ONIOM. We therefore suggest that the DSD-PBE-P86/M06-2X combination would also be appropriate when it is used with the ONIOM technique. For the investigation of large peptides for which the application of even hybrid DFT may represent a challenge, the use of a three-layer protocol may be desirable.

Thermodynamics and Kinetics of α-Hydrogen Abstractions. Having identified appropriate theoretical protocols for the study of α-abstraction reactions of amino acids and peptides, we now briefly turn our attention to the chemical aspects of these reactions. In order to more accurately locate the transition structures using the IRCmax procedure, we have adopted a refined approach recommended previously.[8c] Thus, for each reaction, we have located the maximum on a reaction path obtained with single-point energy calculations at the DSD-PBE-P86/6-31+G(3df,2d,2p) level on the BHandH-LYP/6-31+G(d,p) IRC. The use of the modest 6-31+G(3df,2d,2p) basis set (2p polarization functions for hydrogen, 2d for first-row and 3df for second-row atoms) has been shown to yield reliable transition structures.[8c]

The 298 K reaction free energies and free energy barriers obtained for the peptide derivatives of the amino acids in this manner are shown in Table 6. We can see that the •OH abstraction reactions are highly exergonic, which can be attributed to the formation of the two stable products, namely water and the captodatively-stablized α-radical. In comparison, reactions with the less reactive •SH radical are only mildly exergonic or near-thermoneutral. The precise difference between the reaction free energies for abstraction by •OH and •SH is the difference between the bond dissociation free energies for H–OH and H–SH. This amounts to 111.3 kJ mol^{-1} at the DSD-PBE-P86/aug'-cc-pVTZ+d level. The associated barriers for abstractions by both •OH and •SH radicals are quite moderate, with values of ~ 20–40 kJ mol^{-1} for •OH abstractions and ~ 40–70 kJ mol^{-1} for •SH abstractions. Thus, the large differences in the reaction energies of ~ 100 kJ mol^{-1} appear to be reflected in the barriers but in a heavily damped manner.

Table 6. DSD-PBE-P86/aug'-cc-pVTZ+d Reaction Free Energies and Free Energy Barriers (kJ mol^{-1}) for α-Hydrogen Abstraction by the •OH and •SH Radicals from the Amino Acid Peptide Derivatives $CH_3C(=O)NH–CH(R)–C(=O)NHCH_3$

	Reaction energies		Barriers	
R	•OH	•SH	•OH	•SH
Ala	–137.2	–25.9	19.3	42.6
Arg	–147.6	–36.3	23.7	39.7
Asn	–118.8	–7.5	31.7	50.1
Asp	–123.7	–12.4	34.2	54.4
Cys	–135.2	–23.9	28.1	47.4
Gln	–135.1	–23.8	28.5	42.2
Glu	–109.6	1.7	31.0	59.9
Gly	–140.6	–29.3	30.1	44.2
His	–109.8	1.5	31.7	55.3
Ile	–113.3	–2.0	23.8	55.7
Leu	–114.4	–3.1	38.6	68.0
Lys	–113.1	–1.8	34.8	58.7
Met	–109.5	1.8	34.3	61.4
Phe	–130.4	–19.1	25.7	52.8
Pro	–108.8	2.5	33.6	54.2
Ser	–101.2	10.1	36.2	62.5
Thr	–119.6	–8.2	17.7	48.8
Trp	–126.2	–14.9	31.0	57.3
Tyr	–127.3	–16.0	25.9	53.6
Val	–111.3	0.0	25.5	57.4

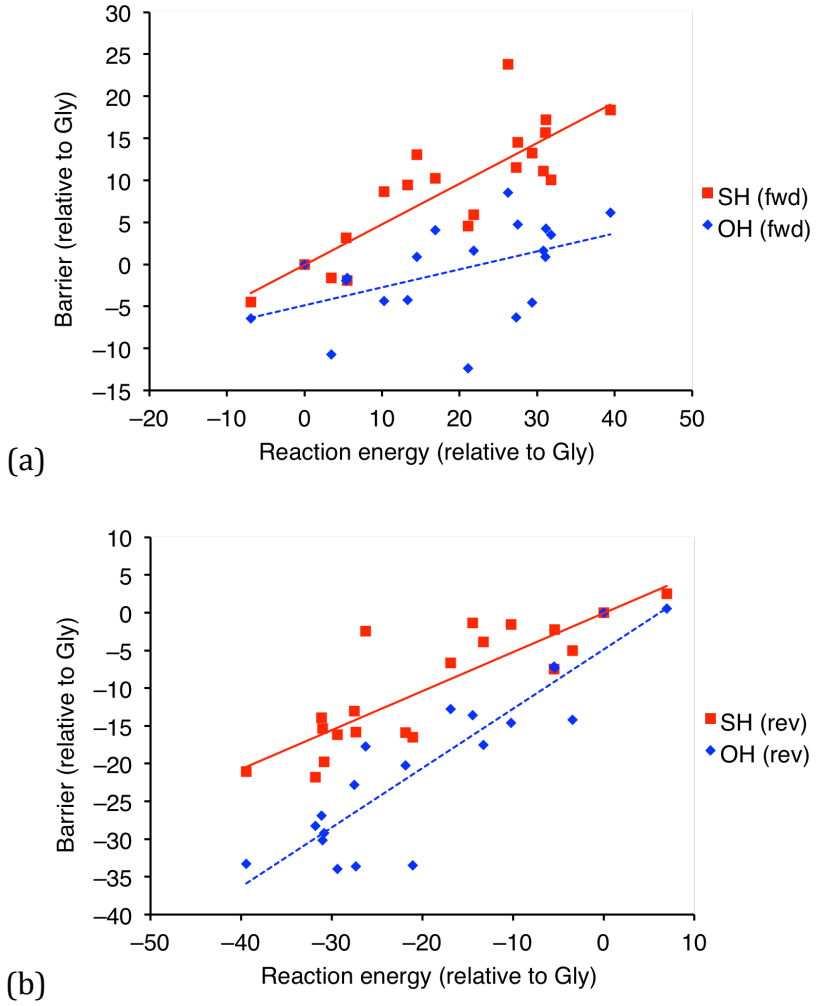

Figure 1. Relationship between the relative free energy barriers and relative reaction free energies (kJ mol^{-1}) for α-abstractions from amino acids by •OH and •SH radicals for (a) forward reactions and (b) reverse reactions.

Are there also qualitative correlations between the barriers for abstractions from the various amino acids and the reaction energies? We have examined this aspect by plotting the relative barriers against the relative reaction energies for both •OH and •SH abstractions, using the values for glycine as the reference. For the forward reactions (Figure 1a), it appears that there is a somewhat better correlation for the reactions with •SH than those with •OH. Indeed, a linear fit of the data for •OH abstractions gives an R^2 value of just 0.24. In comparison, the corresponding R^2 value for the reactions with •SH is 0.69.

It is noteworthy that the slopes of the linear fits can be considered a measure of the degree to which the thermodynamics (reaction energies) is reflected in the kinetics (barriers). Thus, the slope of 0.48 for •SH abstractions suggests that the barriers for these reactions are influenced by the reaction energies to a larger extent than •OH abstractions, for which the slope of the fit is 0.24. These findings are in line with the reactions of •OH being highly exergonic and the transition structures therefore expected to be earlier than those for •SH, with the thermodynamics consequently having less impact on the kinetics. Consistent with this argument, the calculated C••H distances in the transition structures for the •OH abstractions have an average value of 1.12 Å, whereas for the corresponding •SH reactions, the average value is 1.42 Å. The smaller thermodynamic effects in the •OH abstraction barriers would then allow other factors, e.g., polar effects, to play a role with an increased significance, thus leading to a less good correlation with the reaction energies.

For the reverse reactions, the highly exergonic •OH abstractions in the forward direction (Table 6) become endergonic abstraction reactions from H_2O by the peptidic-amino-acid radicals. In these cases, the reaction energies themselves contribute significantly to the barriers. As we can see from Figure 1b, this leads to the abstraction barriers forming a fairly good linear correlation with the corresponding reaction energies. The R^2 value for the linear fit is 0.81 in this case. For the abstraction reactions from H_2S, the corresponding correlation is also quite good, with an R^2 value of 0.72. The slope for the correlation for the H_2O reactions is 0.79, whereas the slope for the H_2S reactions is 0.52. The larger influence of the reaction energies on the H_2O reaction barriers when compared with the H_2S reactions is consistent with the larger endergonicity of H_2O reactions.

Concluding Remarks

In the present study, we have investigated the performance of a range of quantum chemistry procedures for the computation of the thermochemistry of α-hydrogen abstraction by •OH and •SH radicals from the full set of amino acids normally found

in proteins, and their peptide derivatives. A number of key findings emerge from our investigation.

1. For •OH abstraction for a set of neutral amino acids, the DSD-PBE-P86 double-hybrid DFT procedure is found to yield barriers and reaction energies in very good agreement with our benchmark high-level W1X-2 values. The economical composite wavefunction procedures G4(MP2)-6X, G4(MP2) and CBS-QB3 also show fairly small deviations from our benchmarks.
2. The performances for the various classes of theoretical methods show an expected trend: non-hybrid DFT ◘ hybrid DFT ◘ double-hybrid DFT ◘ composite procedures. The differences in performance are largely associated with systematic deviations, which can then be exploited to obtain accurate relative quantities using less demanding methods.
3. Further examination using •OH and •SH abstractions of the α-hydrogen for the full set of peptide derivatives of the amino acids shows generally fair agreement between DSD-PBE-P86, the DuT-D3 double-hybrid DFT, and the G4(MP2)-6X composite procedures. We believe that this is indicative of a degree of robustness in the use of these methods for the study of hydrogen-abstraction reactions of amino acids, and reinforces our findings on neutral amino acids.
4. The use of lower-level methods for the calculation of absolute values for the barriers and reaction energies yields less good agreement with DSD-PBE-P86. However, when one considers relative instead of absolute values, even the least costly MN12-L non-hybrid DFT procedure gives a performance that is quite comparable to that for the highest-level G4(MP2)-6X and DSD-PBE-P86 procedures.
5. We have examined a number of multi-layer schemes for the calculation of reaction energies and barriers for the α-abstraction reactions of the peptide derivatives of the amino acids. We find that accurate values for the absolute reaction energies and barriers can be obtained when a "core" of glycine plus the abstracting radical is treated by DSD-PBE-P86, and the substituent effects of the side chain and peptide derivatisation are evaluated with M06-2X. We propose

that such a combination can also be applied effectively in formal multi-layer methodologies such as ONIOM for the study of these systems.

6. Correlation between the barriers and corresponding reaction energies for abstractions by •OH or •SH radicals is best for reactions that are either endergonic or near-thermoneutral.

Supporting Information

Optimized [BHandH-LYP/6-31+G(d,p)] or IRCmax [DSD-PBE-P86/aug'-cc-pVTZ+d//BHandH-LYP/6-31+G(d,p)] geometries of the relevant species in xyz format contained in a single zip archive (amino_acid_peptide_geom.zip), zero-point vibrational energies, thermal corrections to enthalpies, and entropies, and electronic energies at the various levels of theory. This material is available free of charge via the Internet at http://pubs.acs.org

Acknowledgments

We gratefully acknowledge funding (to L.R. and C.J.E.) from the Australian Research Council (ARC) and generous grants of computer time (to L.R.) from the National Computational Infrastructure (NCI) National Facility and Intersect Australia Ltd.

---

1 Garrison, W. M. *Chem. Rev.* **1987**, *87*, 381–398.

2 (a) Davies, M. J.; Dean, R. T. *Radical-Mediated Protein Oxidation: From Chemistry to Medicine*; Oxford University Press: New York, 1997. (b) Hussain, S. P.; Hofseth, L. J.; Harris, C. C. *Nat. Rev. Cancer* **2003**, *3*, 276–285. (c) Mattson, M. P. *Nature* **2004**, *430*, 631–639.

3 For a review of experimental work, see: (a) Viehe, H. G.; Janousek, Z.; Merenyi, R.; Stella, L. *Acc. Chem. Res.*, **1985**, *18*, 148–154. For theoretical studies, see for example: (b) Rauk, A.; Yu, D.; Taylor, J.; Shustov, G. V.; Block, D. A.; Armstrong, D. A. *Biochemistry* **1999**, *38*, 9089–9096. (c) Croft, A. K.; Easton, C. J.; Radom, L. *J. Am. Chem. Soc.* **2003**, *125*, 4119–4124. (d) Hioe, J.; Savasci, G.; Brand, H; Zipse, H. *Chem. Eur. J.* **2011**, *17*, 3781–3789.

4 (a) Moore, B. N.; Julian, R. R. *Phys. Chem. Chem. Phys.* **2012**, *14*, 3148–3154. (b) Hioe, J.; Mosch, M.; Smith, D.; Zipse, H. *RSC Adv.* **2013**, *3*, 12403–12408.

5 (a) For a review, see: Easton, C. J. *Chem. Rev.* **1997**, *97*, 53–82. See also: (b) Watts, Z. I.; Easton, C. J. *J. Am. Chem. Soc.* **2009**, *131*, 11323-11325.

6 See for example: Russell, G. A. In *Free Radicals*; Kochi, J. K., Ed.; Wiley: New York, 1973, Vol. 1, Chapter 7, pp 275–331.

7 See for example: (a) Pross, A.; Yamataka, H.; Nagase, S. *J. Phys. Org. Chem.* **1991**, *4*, 135–140. (b) Taylor, M. S.; Ivanic, S. A.; Wood, G. P. F.; Easton, C. J.; Bacskay, G. B.; Radom, L. *J. Phys. Chem. A* **2009**, *113*, 11817–11832.

8 (a) Chan, B.; Radom, L. *Theor. Chem. Acc.* **2011**, *130*, 251–260. (b) O'Reilly, R. J.; Chan, B.; Taylor, M. S.; Ivanic, S.; Bacskay, G. B.; Easton, C. J.; Radom, L. *J. Am. Chem. Soc.* **2011**, *133*, 16553–16559. (c) Chan, B.; Radom, L. *J. Phys. Chem. A* **2012**, *116*, 3745–3752. (d) Chan, B.; O'Reilly, R. J.; Easton, C. J.; Radom, L. *J. Org. Chem.* **2012**, *77*, 9807–9812. (e) Amos, R. I. J.; Chan, B.; Easton, C. J.; Radom, L. *J. Phys. Chem. B* **2015**, *119*, 783–788. (f) Chan, B.; Easton, C. J.; Radom, L. *J. Phys. Chem. A* **2015**, *119*, 3843–3847.

9 See for example: (a) Peverati, R.; Truhlar, D. G. *Phys. Chem. Chem. Phys.* **2012**, 16187-16191. (b) Goerigk, L.; Grimme, S. *WIREs Comput. Mol. Sci.* **2014**, *4*, 576–600.

10 See for example: (a) Zipse, H. In *Radicals in Synthesis I: Methods and Mechanisms*; Gansauer, A., Ed.; Topics in Current Chemistry; Springer-Verlag: Berlin, 2006; Vol. 263, pp 163–189. (b) Lin, C. Y.; Hodgson, J. L.; Namazian, M.; Coote, M. L. *J. Phys. Chem. A* **2009**, *113*, 3690–3697. (c) Noble, B. B.; Coote, M. L. *Int. Rev. Phys. Chem.* **2013**, *32*, 467–513.

11 Koch, W.; Holthausen, M. C. *A Chemist's Guide to Density Functional Theory, 2nd Ed.*; Wiley: New York, 2001.

12 Jensen, F. *Introduction to Computational Chemistry, 2nd Ed.*; Wiley: Chichester, 2007.

13 Frisch, M. J.; Trucks, G. W.; Schlegel, H. B.; Scuseria, G. E.; Robb, M. A.; Cheeseman, J. R.; Scalmani, G.; Barone, V.; Mennucci, B.; Petersson, G. A.; et al. *Gaussian 09, Revision C.03*; Gaussian, Inc.: Wallingford CT, 2009.

14 Neese, F. *WIREs Comput. Mol. Sci.* **2012**, *2*, 73–78.

15 Petersson, G. A. In *Computational Thermochemistry: Prediction and Estimation of Molecular Thermodynamics*; Irikura, K. K., Frurip, D. J., Eds.; ACS Symposium Series 677; American Chemical Society: Washington D. C., 1998, pp 237–266.

16 Tarnopolsky, A.; Karton, A.; Sertchook, R.; Vuzman, D.; Martin, J. M. L. *J. Phys. Chem. A* **2008**, *112*, 3–8.

17 Merrick, J. P.; Moran, D.; Radom, L. *J. Phys. Chem. A* **2007**, *111*, 11683–11700.

18 Yuan, Y.; Mills, M. J. L.; Popelier, P. L. A.; Jensen, F. *J. Phys. Chem. A* **2014**, *118*, 7876–7891.

19 Chan, B.; Radom, L. *J. Chem. Theory Comput.* **2012**, *8*, 4259–4269.

20 Curtiss, L. A.; Redfern, P. C.; Raghavachari, K. *J. Chem. Phys.* **2007**, *126*, 084108.

21 Chan, B.; Deng, J.; Radom, L. *J. Chem. Theory Comput.* **2011**, *7*, 112–120.

22 Curtiss, L. A.; Redfern, P. C.; K. Raghavachari, K. *J. Chem. Phys.* **2007**, *127*, 124105.

23 Henry, D. J.; Sullivan, M. B.; Radom, L. *J. Chem. Phys.* **2003**, *118*, 4849–4860.

24 Montgomery Jr., J. A.; Frisch, M. J.; Ochterski, J. W.; Petersson, G. A. *J. Chem. Phys.* **2000**, *112*, 6532–6542.

25 Goerigk, L.; Grimme, S. *J. Chem. Theory Comput.* **2011**, *7*, 291–309.

26 Chan, B.; Radom, L. *J. Chem. Theory Comput.* **2011**, *7*, 2852–2863.

27 Kozuch, S.; Martin, J. M. L. *J. Comput. Chem.* **2013**, *34*, 2327–2344.

28 Zhao, Y.; Truhlar, D. G. *J. Phys. Chem. A* **2005**, *109*, 5656–5667.

29 Chai, J.-D.; Head-Gordon, M. *J. Chem. Phys.* **2008**, *128*, 084106.

30 Zhao, Y.; Truhlar, D. G. *Theor. Chem. Acc.* **2008**, *120*, 215–241.

31 Zhao, Y.; Truhlar, D. G. *J. Chem. Phys.* **2006**, *125*, 194101.

32 Peverati, R.; Truhlar, D. G. *Phys. Chem. Chem. Phys.* **2012**, *10*, 13171–13174.

33 Chan, B.; Morris, M.; Radom, L. *Aust. J. Chem.* **2011**, *64*, 394–402.

34 Chan, B.; Radom, L. *J. Phys. Chem. A* **2012**, *116*, 4975–4986.

35 Chan, B.; Radom, L. *J. Phys. Chem. A* **2013**, *117*, 3666–3675.

36 *NIST Chemistry WebBook*; Linstrom, P. J.; Mallard, W. G., Eds.; NIST Standard Reference Database Number 69; National Institute of Standards and Technology, Gaithersburg MD 20899, 2011 (http://webbook.nist.gov).

37 Dapprich, S.; Komáromi, I.; Byun, K. S.; Morokuma, K.; Frisch, M. J. *J. Mol. Struct.* **1999**, *462*, 1–21.